Yussef G. I. ACLE[1], Francisco D. FREITAS[1], João Y. ISHIHARA[1]

Department of Electrical Engineering, University of Brasilia, Brasilia-DF, Brazil (1)

doi:10.15199/48.2017.07.24

Effectiveness evaluation of the Lagrangian modified barrier function method on solving the optimal reactive power flow considering time-varying power demand

Abstract. *This paper proposes the application of the Lagrangian Modified Barrier Function (LMBF) method to solve the Optimal Reactive Power Flow (ORPF) problem in electrical power systems considering time-varying power demand. Some proper adaptations were accomplished to the LMBF method and evaluated on a three-bus test system for different power demand conditions. Even for stressed operational conditions the method demonstrated appropriated characteristics of convergence and precision.*

Streszczenie. *Opisano wykorzystanie funkcji Lagrangian Modified Barrier Function (LMBF) do rozwiązania problemu optymalnego przepływu mocy biernej w sieci elektrycznej uwzględnmiając zmieniające się w czasie zapotrzebowanie na energię.* ***Ocena skuteczności funkcji Lagrangian Modified Barrier Function do rozwiązania problemu optymalnego przepływu mocy biernej w sieci elektrycznej uwzględnmiając zmieniające się w czasie zapotrzebowanie na energię***

Keywords: Lagrangian modified barrier function method, optimal reactive power flow, random power demand
Słowa kluczowe: funkcja Lagrangian Modified Barrier Function (LMBF) ,.optymalny przepływ mocy biernej

Introduction

The Optimal Power Flow (OPF) problem has been addressed in several nonlinear programming (NL) studies in order to optimize allocation of resources and enhance electrical system operation. A specific similar problem is the Optimal Reactive Power Flow (ORPF), where the decision variables are directly involved in reactive power control analysis [1].

In order to tackle NL optimization and satisfy all equality and inequality constraints, several strategies and approaches were developed, such as the use of barriers, penalties, Lagrangian functions, etc.

Compared to classical barriers, modified barrier methods [2] have important advantages, as their finite convergence allows solutions on feasible region boundaries, and they are smooth and finite in a neighbourhood of the optimum.

As presented in [1], the Lagrangian Modified Barrier Function (LMBF) method combines the best qualities of modified barrier and primal-dual interior point methods. LMBF depends on auxiliary variables and modified logarithmic barrier to deal with inequalities in the ORPF. In this sense, all original inequality constraints are transformed into equalities and a specific Lagrangian function is associated to the ORPF. A set of nonlinear equations is generated, when first order necessary optimal conditions [3] are applied on this Lagrangian function. Then the ORPF is solved by an adaptation of Newton's method. The effectiveness of the LMBF on solving the ORPF on deterministic constant power demand conditions was verified in [1]. Also in [4], the method was adopted for controlling the power injected into a system by wind farm.

In this paper, we propose to apply the LMBF [1] technique to the ORPF problem, where the power demand changes along the time. The main motivation is justified since random variation of electrical quantities is a concern mainly due to the insertion of mixed sources in modern power systems, such as wind penetration in the distribution networks [5]. In the formulation problem, the active power losses in the system [6] are assumed as objective function. To verify the performance of the methodology, some experiments are assessed in a 3-bus test system. With this goal, several numerical tests were performed under different and stressed demand conditions. The Lagrangian gradient infinity norm was used as stop criterion for convergence. The required number of iterations to achieve determined precision and the suitability of LMBF method for real-time applications are analysed.

The Lagrangian Modified Barrier Function Method

The main idea in using barriers in optimization problems is to initially solve an alternative problem as it was unrestricted, because the barrier, if properly set, does not allow violation of constraints. Then, the effect of the presence of the barrier itself diminishes as its parameters are updated, leading to the original problem approximate solution.

Let $f_c(x)$ be a scalar cost (objective) function, with x a column vector of N decision variables. Also, let $h_i(x)$ and $g_j(x)$ be the i-th of N_{eq} equality constraints and the j-th of N_{ineq} inequality constraints, respectively. The original NL problem is stated as:

$$\text{(1)} \quad \begin{cases} \text{Minimize } f_c(x), \text{ subject to} \\ h_i(x) = 0, i = 1, ..., N_{eq} \\ B_{2j} \le g_j(x) \le B_{2j-1}, \quad j = 1, ..., 0.5 \times N_{ineq} \end{cases}$$

where $B=[B_1,\cdots,B_{ineq}]^T$ is an array of N_{ineq} bounds, where odd and even entries stand for upper and lower bounds, respectively.

After the modification of problem (1) consisting of addition of N_{ineq} slack variables from a column array s, the problem is rewritten as [1]:

$$\text{(2)} \quad \begin{cases} \text{Minimize } f_c(x), \text{ subject to} \\ h_i(x) = 0, i = 1, ..., N_{eq} \\ g_j(x) - B_j - (-1)^k s_j = 0, \quad j = 1, ..., N_{ineq} \\ s_k \ge 0, \quad k = 1, ..., N_{ineq} \end{cases}$$

In (2), index k odd means inequality related only to upper limits, while even is for lower limits. The LMBF technique was implemented with logarithmic Frisch modified barrier [2]. For instance, if $s_1 \ge 0$, then $\ln(\mu^{-1}s_1+1) \ge 0$, where $\mu > 0$ is the barrier parameter. Applying the method proposed in [2], the system (2) is transformed into:

$$\text{(3)} \quad \begin{cases} \text{Minimize } f_c(x), \text{ subject to} \\ h_i(x) = 0, i = 1, ..., N_{eq} \\ g_j(x) - B_j - (-1)^k s_j = 0, \quad j = 1, ..., N_{ineq} \\ \mu \ln\left(\mu^{-1} s_k + 1\right) \ge 0, \quad k = 1, ..., N_{ineq} \end{cases}$$

A modified barrier Lagrangian is associated with (3) as follows:

$$L(x,\lambda,s,\pi) = f_c(x) + \mu\sum_{i=1}^{N_{ineq}} u_i \ln(\mu^{-1}s_i + 1) + \\ +\sum_{j=1}^{N_{eq}} \lambda_j h_j + \sum_{k=1}^{N_{ineq}} \pi_k(g_k(x) - B_k - (-1)^k s_k) \quad (4)$$

where λ_j, π_k are entries of column vectors of the original equality constraints Lagrange multipliers and transformed inequality constraints Lagrange multipliers, respectively. In this implementation, only one barrier parameter, μ, is used, but N_{ineq} different parameters could be used in (4). The term u_i is the i-th element of the vector u of barrier Lagrange multipliers, artificially created with the barrier.

Once the Lagrangian function in (4) is established, optimal first order necessary conditions are applied on it [3], generating a set of nonlinear equations:

$$\nabla L(x,\lambda,s,\pi) = \frac{\partial L}{\partial d} = \mathbf{0} \in \mathbb{R}^{(N+N_{eq}+2N_{ineq})} \quad (5)$$

where d=[x^T, λ^T, s^T, π^T]^T is a direction search vector. Notice that no derivative of L with respect to u is taken, as it is updated with a separate rule.

The equations in (5) with derivatives with respect to the original decision variables x represent the optimality of the problem regarding those variables. The equations involved in the differentiation of λ and π are related to the original equality constraints in (1) and the transformed inequality constraints in (2), respectively. Also, the equations with the derivatives with respect to s are involved with the modified logarithmic barrier. They must be satisfied for eliminating the effect of the presence of the barrier in the ORPF, and also for finding the original problem (1) solution.

Newton's method is used to solve (5). With this aim, at each iteration γ, the Hessian matrix defined by W=$\partial\nabla L/\partial d$ must be calculated. We need to solve the linear system $W\times\Delta d$ = -$\nabla L(x,\lambda,s,\pi)$, where Δd=[Δx^T, $\Delta\lambda^T$, Δs^T, $\Delta\pi^T$]^T is an array of increments that is calculated to update d. However, its use is not straightforward as considered for the traditional Newton's method. Then, few adaptations are required. Actually, the update is of the form [1]:

$$\begin{aligned} x^{(\gamma+1)} &= x^{(\gamma)} + \alpha_p \Delta x^{(\gamma)} \\ s^{(\gamma+1)} &= s^{(\gamma)} + \alpha_p \Delta s^{(\gamma)} \\ \lambda^{(\gamma+1)} &= \lambda^{(\gamma)} + \alpha_d \Delta\lambda^{(\gamma)} \\ \pi^{(\gamma+1)} &= \pi^{(\gamma)} + \alpha_d \Delta\pi^{(\gamma)} \end{aligned} \quad (6)$$

where α_p and α_d are the primal and dual step sizes used in the update. They must be properly selected in order to avoid that $s_i < 0$ or $(-1)^i\pi_i < 0$, i=1,…,N_{ineq}. The barrier parameter is updated as [1]:

$$\mu^{(\gamma+1)} = \mu^{(\gamma)}\left(1 - \frac{\rho}{\sqrt{N_{ineq}}}\right) \\ \rho = \max_{s_j>0}\left(\frac{1}{\mu^{-1}s_j+1}\right), j = 1,...,N_{ineq} \quad (7)$$

The barrier Lagrange multipliers u are updated as follows [2]:

$$u^{(\gamma+1)} = u^{(\gamma)}\frac{u^{(\gamma)}\mu^{(\gamma+1)}}{s^{(\gamma+1)}+\mu^{(\gamma+1)}} \quad (8)$$

The first iteration of Newton's method can start with an unfeasible solution, but must be initialized with $s > -\mu$ [1]. The stop criterion used was based on the Lagrangian Gradient Precision (LGP) required for convergence. In this case, the infinity norm $||\nabla L(x,\lambda,s,\pi)||_\infty \le$ LGP . Also, it is possible to constrain the process to a fixed maximum number of iterations (MaxIt).

The adoption to use the term $||\nabla L(x,\lambda,s,\pi)||_\infty$ in the stop criterion not only meet optimality equations, but also simultaneously guarantees that: all bounds are fulfilled; equality constraints (in the case of ORPF, the traditional power flow equations [6]) are satisfied; and the original problem (1) has been solved.

LMBF applied on time-varying power demand ORPF

The traditional power flow problem analysis assumes that the load has fixed parameter. For instance, the load can be composed of constant portions of impedance (Z), current (I) and power (P), the so called ZIP model [6]. However, considering practical conditions, the status (on/off) of loads is changing continuously as a function of time. Since we cannot control the status of loads, in the sense that a power source must always be available to supply them, the loads can be considered changing randomly in time. As a consequence, the system operational conditions might be evaluated stochastically.

The power demand data is considered to be received from N_s samples, as a discrete load evolution along time, and will be referred along the text as *Power Samples*. This is intended to simulate the real-time monitoring of measured load. Each sampling time a new power sample is received, the applied LMBF must be able to follow the change in power samples, and provide an evolution of optimal solutions as well.

Algorithm 1 presents the basic procedures of LMBF method when applied to solve the optimal reactive power flow in an electrical system with time-varying power demand.

Algorithm 1 – LMBF applied in time-varying demand ORPF

INPUT:	Power Samples, electrical system model data, parameter values, bounds
OUTPUT:	Optimal solution for the ORPF
1.	Initialization
2.	Do k=1,2 ..., N_s
3.	Receive k-th power sample
4.	update $L(x,\lambda,s,\pi)$ in (4)
5.	If (k > 1), start with solution from previous power sample and reset μ and u values
6.	Compute $\nabla L(x,\lambda,s,\pi)$ and set γ=0
7.	While ($\|\|\nabla L(x,\lambda,s,\pi)\|\|_\infty$>LGP) AND ($\gamma \le$ MaxIt) do
8.	Compute Hessian W
9.	Solve $W\times\Delta d$ = -$\nabla L(x,\lambda,s,\pi)$
10.	update d with (6)
11.	update barrier parameters with (7) and (8)
12.	update γ as γ:= γ+1
13.	Compute $\nabla L(x,\lambda,s,\pi)$ with updated information
14.	End While
15.	End Do k

Line 5 in Algorithm 1 plays a key role, since starting from the previous solution and setting μ and u properly can significantly enhance the number of iterations required to achieve the desired LGP. On the other hand, setting very low values for this target index can lead to the LMBF inability to solve the problem, or it may converge to a wrong answer.

In the ORPF, the decision variables are x=[θ^T,V^T]^T, where θ and V are, respectively, arrays of phase angle and voltage magnitude of all buses, except for the angular reference, which is fixed.

In this case, the equations in (5) with differentiation in λ specifically lead to the traditional power flow equations [5,7], which must be satisfied in the optimization process. These equations are the balance of active power injection, at PQ and PV buses, and reactive power injection, at PQ buses:

$$\Delta P_k(\theta,V) = P_k^{sp} - V_k \sum_{m\in\Omega_k} V_m[G_{km}\cos(\theta_{km}) + B_{km}\sin(\theta_{km})] = 0, \quad k = 1,2,\cdots,(N_{PQ}+N_{PV}) \tag{9}$$

$$\Delta Q_j(\theta,V) = Q_j^{sp} - V_j \sum_{m\in\Omega_j} V_m[G_{jm}\sin(\theta_{jm}) - B_{jm}\cos(\theta_{jm})] = 0, \quad j = 1,2,\cdots,N_{PQ} \tag{10}$$

where P_k^{sp} is the specified active power at buses of type PQ and PV, Q_k^{sp} is the specified reactive power at PQ buses, θ_{km} stands for the angular deviation $\theta_{km}=\theta_k-\theta_m$, N_{PQ} and N_{PV} are the number of PQ and PV buses, respectively. The terms G_{km} and B_{km} are, respectively, the real and imaginary parts of the elements from the bus nodal admittance matrix, $\boldsymbol{Y_{bus}=G+jB}$ [6], where j is the imaginary unit. The symbol Ω_i means a subset of buses with physical connection at bus i.

The objective function assumed was defined as the total active power losses in the system, that is, the sum of all active power dissipation in the network interconnections:

$$f_c(\theta,V) = \sum_{(k,m)\in\Omega_L} g_{km}(V_k^2 + V_m^2 - 2V_kV_m\cos(\theta_{km})) \tag{11}$$

where g_{km} is the series admittance in the branch between bus k and bus m, Ω_L is the subset of all branches in the system.

Test system

To demonstrate the efficacy of the methodology presented in this paper, experiments are carried out on a power system. The electrical test system considered consists in a three-bus network, extracted from [1]. Figure 1 exhibits the one-line diagram of the system. Bus 1 is the slack (swing) bus [6], where the angular reference is fixed. Bus 2 is a PV bus type with active power injection. The load that dictates the power demand $P_{3,L}+jQ_{3,L}$ is connected to bus 3, a PQ bus. The interconnection between two buses is modelled by single admittance y_{13} and y_{23}.

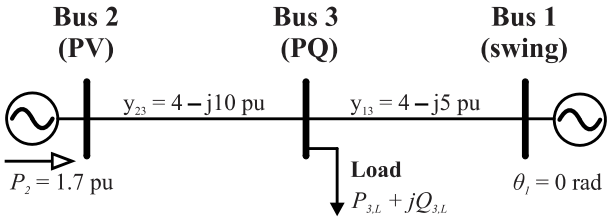

Fig.1. The three-bus system model

The active and reactive power demand at bus 3, $P_{3,L}$ and $Q_{3,L}$, are treated as inputs of the LMBF method. The load could be modelled by different functions of electrical quantities. However, in the experiments each power sample is treated as a constant power load. This means that the value of power demand is not influenced by the values of voltage (magnitude and phase) at any of the buses. Considering this, the analytical expressions for gradient ∇L and Hessian W will not change. Hence, lines 8 and 13 of Algorithm 1 can be accomplished with updated values instead of new computations for this aim.

The voltage magnitudes at PV and swing buses, usually fixed in the traditional power flow problem [6], are left as degrees of freedom to be determined in the optimization process.

All voltage magnitudes [V_1, V_2, V_3] and reactive power injected in bus 2, Q_2, have upper and lower bounds, giving N_{ineq}=8. In fact, Q_2 is:

$$Q_2(\theta,V) = V_2V_3[G_{23}\sin(\theta_{23}) - B_{23}\cos(\theta_{23})] \tag{12}$$

Since $N_{PQ} = N_{PV} = 1$, there are 3 traditional power flow equations for this system, that is $N_{eq} = 3$. Also, the problem in (5) results in $N+N_{eq}+2N_{ineq}$=24, which is the order of the Lagrangian gradient and the order of the Hessian matrix. We emphasize that experiments with larger systems could be carried out. Our preference for a simple test system is to facilitate the demonstration of the methodology and also to provide tools for easy reproduction of results by the users.

Numerical Experiments and Results

Several experiments were accomplished based on the test system presented in Fig. 1. For all experiments the tolerance MaxIt was set as a free value (very large value). Only power demand at bus 3 is supposed to change, while the electrical network remains unaltered. So, the expression of the Lagrangian gradient and Hessian are kept constant. Although computation time may differ from every machine, for purposes of reference Table 1 furnishes figures of simulations. The data include the CPU mean time required for performing all computations considering a set of N_s samples. The statistics also highlights the standard deviation of the CPU time at each iteration and the worst case for a single iteration, after 10^6 iterations.

Table 1. Iteration computational figures after 10^6 iterations

CPU mean value (second)	2.4283×10^{-4}
CPU standard deviation (second)	1.0346×10^{-4}
CPU time worst case (second)	$\sim1\times10^{-3}$

All experiments have been initialized with flat start condition (phase and magnitude voltages at 0 rad and 1 pu, respectively). The barrier parameters initial values were μ=0.1 and u set as an array of ones. For each new power sample evaluated, the initial values of μ and u are used.

Table 2 presents the possible cases of bounds studied in this work. The case 2 is the one that presents broader limits.

Table 2. Feasible intervals for different cases studied in this work

Case	Bound	V_1	V_2	V_3	Q_2
1	Lower	0.95	0.95	0.94	-1.30
	Upper	1.05	1.10	1.05	1.30
2	Lower	0.90	0.90	0.90	-2.00
	Upper	1.10	1.10	1.10	2.00
3	Lower	0.95	0.95	0.90	-1.30
	Upper	1.08	1.10	1.05	0.90

In the following, details are exposed about each experiment considering power demand characteristics. For each scenario the power demand has a Gaussian noise $\mathcal{N}(\eta,\sigma^2)$, where η is the mean and σ, the standard deviation [7]. The experiments were assessed for ten scenarios ($\mathbf{S}_i$, i=1,⋯,10) and two accuracy situations: LGP 10^{-4} and 10^{-8}. Except for the scenario $\mathbf{S_{10}}$ with N_s=288 samples, all other simulations had 1440 power demand samples. Evidently, the sample interval period between two samples is set accordingly the power system utility. Then, except for the scenario $\mathbf{S_{10}}$, we supposed that an optimal power flow is solved (new power demand sample) considering an interval of one minute. Note that smaller or higher sampling intervals can be established without compromising the methodology adopted in this work.

$\mathbf{S_1}$: active power constant at 1 pu and constant inductive power factor (PF) 0.92 plus noise $\mathcal{N}(0,0.1^2)$ added to both active and reactive powers. Bound case 1 from Table 2 is assumed.

$\mathbf{S_2}$: same as test 1, but with noise replaced by $\mathcal{N}(0,0.3^2)$.

$\mathbf{S_3}$: $Q_{3,L}$ constant at 1 pu and $P_{3,L}$ =2k/1440, k=1,…,1440, where k means an index for sampling time, in such way that

the active power is modelled as a ramp function with the final value 2 pu. Bound case 1 from Table 2 is assumed.
S_4: $P_{3,L}$ constant at 1 pu and $Q_{3,L}$ = -1 + 2k/1440, k=1,…,1440. Bound case 1 from Table 2.
S_5: $Q_{3,L}$ constant at 1 pu and $P_{3,L}$ = 1 + (k/1440)×(-1)^k pu, k=1,…,1440. Bound case 1 from Table 2.
S_6: $Q_{3,L}$ =0.5 × P_3 and $P_{3,L}$ = 1 + (k/1440)×(-1)^k, k=1,…,1440,. Bound case 1 from Table 2.
S_7: same as test 6, but with Bound case 2 from Table 2.
S_8: $P_{3,L}$ = 1 - cos(2πk/1440), k =1,…,1440, and constant inductive PF at 0.92. Added noise $\mathcal{N}(0,0.2^2)$ to both active and reactive powers. Bound case 1 from Table 2.
S_9: same as test 8, but with bound case 2 from Table 2.
S_{10}: $P_{3,L}$ based on data acquired on [8] and constant inductive PF at 0.92. Added noise $\mathcal{N}(0,0.02^2)$ to both active and reactive powers. Bound case 3 from Table 2.

For each power load sample, a number of iterations is identified aiming a given accuracy LGP, which is required for an optimal power flow. At the end of the process statistics of the number of iterations required by sample are evaluated. The numerical results regarding the number of iterations are displayed in Table 3 by considering two LGP values.

Table 3. Results regarding number of iterations for each scenario S_i

S_i	Lagrangian gradient precision	Mean number of iterations	Standard deviation of iterations	Maximum number of iterations
1	10^{-4}	26.1021	3.3811	50
	10^{-8}	50.6722	6.7244	118
2	10^{-4}	38.9854	20.8672	159
	10^{-8}	88.2535	86.0014	1344
3	10^{-4}	39.3000	13.3182	86
	10^{-8}	94.0139	88.2281	1306
4	10^{-4}	40.5194	24.7685	157
	10^{-8}	90.4194	104.7045	2067
5	10^{-4}	39.3090	13.2648	88
	10^{-8}	94.2708	92.9552	1786
6	10^{-4}	**48.9701**	56.7408	**1153**
	10^{-8}	**104.4181**	142.4373	**3026**
7	10^{-4}	16.6708	1.5918	23
	10^{-8}	31.7396	4.1431	46
8	10^{-4}	**51.8201**	54.2751	**681**
	10^{-8}	**112.5903**	153.3188	**3314**
9	10^{-4}	18.5306	6.1921	86
	10^{-8}	36.7521	18.0679	314
10	10^{-4}	36.1563	31.8921	364
	10^{-8}	73.6493	75.7221	772

In Table 3, experiments on scenarios **S_6** and **S_8** were the most stressful to the system, and required the highest number of iterations.

The bounds must be set accordingly, since narrower intervals may require more iterations as usual. See for instance results exhibited in Figure 2 for scenarios **S_8** and **S_9**, for LGP 10^{-4}. Similar observations may apply to a comparison between scenarios **S_6** and **S_7** in Table 3. Furthermore, very strict bounds may lead to an unfeasible operating point, where (1) has no solution.

Figure 3 presents the power demand evolution for the scenarios **S_8** and **S_9**. The plots highlight the severe disturbance caused by the presence of noise characterizing the power load. On the other hand, Figure 4 illustrates the evolution of voltage magnitudes on scenario **S_8** for LGP 10^{-8}. It can be seen that V_1 remains between its bounds of 0.95 pu and 1.05 pu, the magnitude V_3 remains between 0.94 pu and 1.05 pu, while V_2 is submitted to its upper bound of 1.10 pu. Clearly, the LMBF was successfully able to find the optimal solutions, even for stressful experiment.

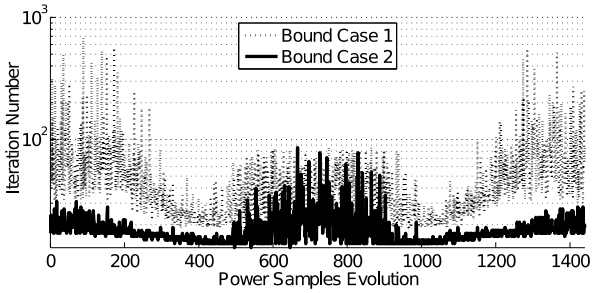

Fig.2. Iteration number evolution on scenarios **S_8** and **S_9**

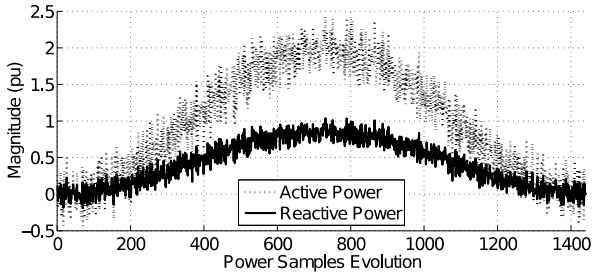

Fig.3. Power demand on scenarios **S_8** and **S_9**

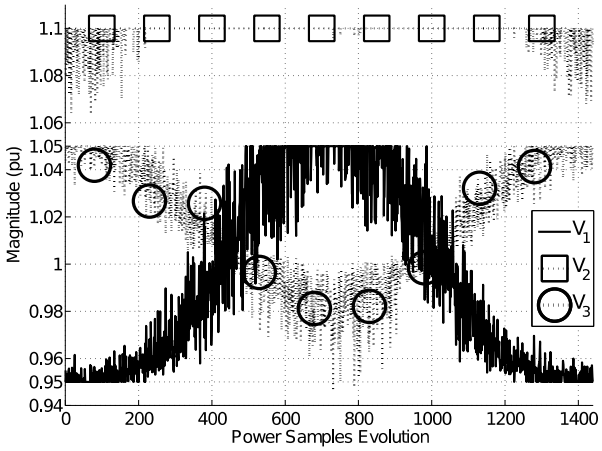

Fig.4. Voltage magnitudes evolution for scenario **S_8**

The daily power demand based on real data acquired from [8] is presented in Figure 5, for the scenario **S_{10}**. For this scenario, a power demand sample is taken at each five minutes, totalizing 288 samples along a day (24 hours, i.e., 1440 minutes). Figure 6 illustrates the evolution of bus voltage magnitudes and Q_2 for this load scenario. It can be seen that Q_2 is set on its upper bound 0.9 pu along the more stressed period observed. Also, V_1 and V_2 also do not exceed their upper bounds.

Figure 7 shows the numerical impact of the required accuracy on the solution of LMBF method. The results are illustrated for experiments based on scenario **S_{10}**. We conclude that for the same power samples, higher values of LGP will require more iterations.

As an alternative procedure, instead of fixing the LGP and counting the number of iterations required for each power sample, the number of iterations is fixed *a priori*, and the value evolution of $||\nabla L(x,\lambda,s,\pi)||_\infty$ is observed. Figure 8 presents the results for the scenario **S_{10}** for three numbers of iterations (10, 40 and 300 iterations). It can be seen that along the period of higher value of power demands more iterations are required than in situations where the system is lesser stressed. This confirmation is verified even for the case when 300 iterations are set. Values of $||\nabla L(x,\lambda,s,\pi)||_\infty$ for 300 iterations are almost the same one obtained for 40 iterations along the more stressed period.

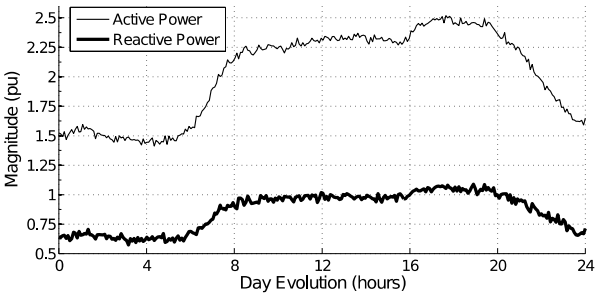

Fig.5. Daily power demand for the scenario **S_{10}** [8]

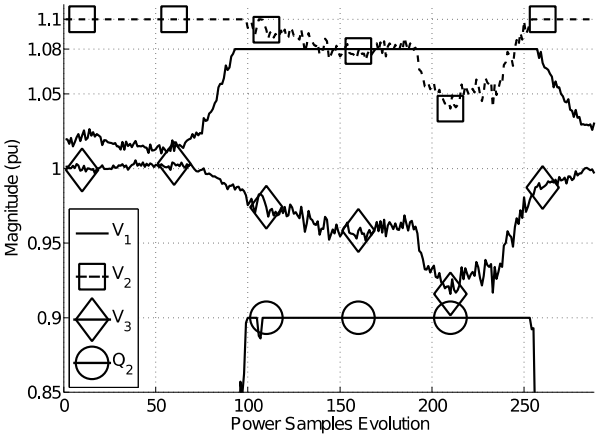

Fig.6. Voltage magnitudes and Q_2 values for the scenario **S_{10}**

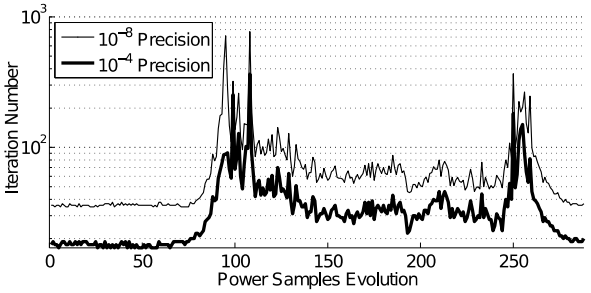

Fig.7. Iteration counts evolution on test 10, for different LGP

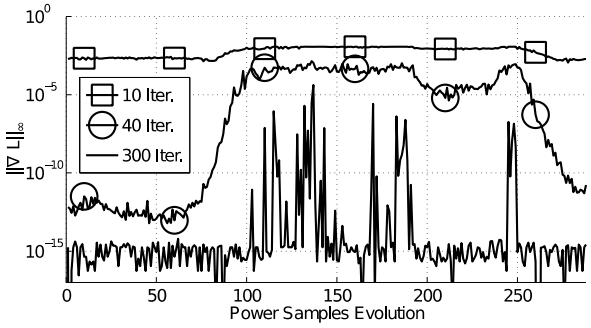

Fig.8. Index $||\nabla L||_\infty$ evolution for the scenario **S_{10}** considering fixed iteration number (10, 40 and 300 iterations)

After performing all experiments, a conservative value for the upper limit of iterations ($MaxIt$), in Algorithm 1, could be established as the maximum number of iterations required for the most stressful experiment, for a given LGP. For example, for LGP 10^{-4}, scenario **S_6** has been characterized as that one which required the highest number of iterations. Then, according to this aspect it would be reasonable to set $MaxIt$ =1153 for future experiments with the same electrical system. In addition, considering the worst case of time demand in Table 1 (1×10^{-3} s), it can be assumed that real-time applications can properly operate within time window of $(1153)\times(1\times10^{-3})$=1.153 second.

For all experiments, it has been verified that the step 9 in Algorithm 1 is the one that demands the highest computational cost. The burden is due to the solution of the linear system $W\times\Delta d = -\nabla L(x,\lambda,s,\pi)$. Then, for large-scale system, the use of newly developed techniques, such as presented in [9], could significantly reduce processing time in the problem. However, the study and details involving this kind of system is out of the scope of the present paper and is objective of another publication.

Conclusions

This paper presented an application of the LMBF method to solve the optimal reactive power flow problem when power demand changes in time.

A set of computational tests were conducted on a three-bus electrical system to evaluate the performance of the proposed methodology, under different voltage and reactive power injection operational conditions and bounds.

In all experiments, the LMBF successfully reached the optimal solutions, although it may have required more iterations for higher precisions, narrower bounds and more stressful power demands. A proper set of parameters can turn this application suitable for real-time operations and monitoring.

In future works, we intend to evaluate the methodology for large scale systems and also include other load models, such as proper modelling of induction motors [6].

***Authors**: Yussef Guardia Ismael Acle, e-mail: yussef.acle@gmail.com, prof. Francisco Damasceno Freitas, e-mail: ffreitas@ene.unb.br, and prof. João Y. Ishihara, ishihara@ene.unb.br, Department of Electrical Engineering, University of Brasilia, CEP:70910-900, Brasilia, DF, Brazil.*

The correspondence address is:
E-mail: yussef.acle@gmail.com

REFERENCES

[1] Sousa, V. A.; Resolution of Reactive Optimal Power Flow Problem Via Method of Lagrangian Modified Barrier Function. Ph.D. Thesis, São Carlos School of Engineering, University of São Paulo, São Carlos, Brazil (2006)

[2] Polyak, R. A.; Modified barrier functions, *Mathematical Programming*, v. 54 (1992), n.2, pp. 177-222

[3] Güler, O.; Foundations of Optimization. Graduate Texts in Mathematics. Springer, New York, NY, USA (2010)

[4] Murari, L. L., Tabares, H. G., Vargas, G. A. L. Belati, E. A, Sousa, V. A., Salles, M. B. C.; Sguarezi Filho, A. J.; Study of transmission system with wind power control and optimal reactive power flow. Przeglad Elektrotechniczny, R. 90, NR 7 (2014), pp. 88-93

[5] Saíz-Marín, E., Lobato, E.; Optimal voltage control by wind farms in distribution networks using regression techniques. Przeglad Elektrotechniczny, R. 88, NR 1a (2012), pp. 117-121

[6] Kundur, P.; Power System Stability and Control, McGraw-Hill Inc, New York, USA (1994)

[7] Meyer, P. L.; Introductory Probability and Statistical Applications, 2nd ed., Addison-Wesley Publishing Company Inc., USA (1970)

[8] Daily Power Demand data acquired from G. B. National Grid Status (GridWatch) Database, courtesy of Elexon portal and Sheffield University, http://www.gridwatch.templar.co.uk/, accessed on Jan 12th, 2017

[9] Fernandes, A. A., Freitas, F. D., Ishihara, J. Y.; Performance assessment of iterative linear methods for the computation of the power flow problem solution, *Przegląd Elektrotechniczny*, 91 (2015), nr 9, pp. 254-258